Preparation and Properties of Novel Polythiophenes Containing 1,3-Dithiol-2-ylidene Moieties

Masatoshi Kozaki, Shoji Tanaka, and Yoshiro Yamashita*

Department of Structural Molecular Science, The Graduate University for Advanced Studies and Institute for Molecular Science, Myodaiji, Okazaki 444, Japan

Received July 26, 1993[⊗]

4-(1,3-Dithiol-2-ylidene)-4*H*-cyclopenta[2,1-*b*;3,4-*b*']dithiophenes **1** and 7-(1,3-dithiol-2-ylidene)-7*H*-cyclopenta[1,2-*b*;4,3-*b*']dithiophenes **2** were prepared by Wittig-Horner or Wittig reactions. The X-ray structural analyses of the parent compounds **1a** and **2a** reveal that both molecules have planar structures with short intermolecular S···S contacts, and **2a** additionally has short intramolecular S···S contacts. They have low oxidation potentials and absorptions in a long wavelength region due to the 1,3-dithiole skeleton. Electrochemical oxidation of **1** and **2** afforded the corresponding polymers **3** and **4**, which have low oxidation potentials. Electrochemically dedoped films of **3** and **4** have interband absorptions at 610–690 nm and 420–590 nm, respectively, in their electronic spectra. Some films of **3** and **4** exhibited high electrical conductivities with doping, for instance, **3c**·$(PF_6^-)_x$, 33 S cm^{-1} and **3e**·$(BF_4^-)_x$, 52 S cm^{-1}. Derivatives **3f–h**, containing linear alkyl chains, were synthesized in order to enhance solubilities in organic solvents and were found to be somewhat soluble in THF and chloroform. Dedoped **3g** showed broad peaks in the ^{1}H NMR spectrum, assigned to the alkyl protons. MNDO-PM3 calculations showed that the torsion angles between the neighbor monomer fragments in the dimers and trimers of **1a** and **2a** are about 30°. However, the oligomers derived from **1a** have more extended conjugated systems than those from **2a**, which was indicated by INDO/1 calculations.

Recently, much work has been devoted to the development of conducting polymers on account of their novel electrical, electrochemical, and optical properties.[1,2] Polythiophene is one of the most widely investigated conducting polymers due to its ready modification and stability in both undoped and doped states.[2-4] Many polythiophene derivatives have been prepared,[4] although their conductivities are rather low compared to that of the parent polythiophene, except for a few derivatives such as polyisothianaphthene (PITN) reported by Wudl et al.[5] Two strategies have been considered to improve the conducting properties. One is to make the polymer structure more defined,[3] and the other is to modify the structure of the monomer.[4] In this connection, we decided to introduce 1,3-dithiole groups into a conductive polymer for four reasons. (i) They induce strong intermolecular interactions through chalcogen–atom contacts as observed in the tetrathiafulvalene (TTF) series.[6] This may result in strong interchain interactions which are useful for the enhancement of charge transport between adjacent chains, as well as for the control of structural order.[7] (ii) The extended π-conjugation and polarization inherent to 1,3-dithiole groups may lead to smaller bandgaps which are favorable for intramolecular electron movement. (iii) The p-doping, conducting states may be stabilized by aromatic 1,3-dithiolium ions formed by oxidation, which is important for preservation of conductivities. (iv) Substituents can be easily introduced to 1,3-dithiole rings in order to modify the characters of polymers. Therefore, we have designed 4-(1,3-dithiol-2-ylidene)-4*H*-cyclopenta[2,1-*b*;3,4-*b*']dithiophenes **1** and 7-(1,3-dithiol-2-ylidene)-7*H*-cyclopenta[1,2-*b*;4,3-*b*']dithiophenes **2** and prepared the corresponding conducting polymers **3**[8] and **4**[9] by an electrochemical method. In these polymers, the 1,3-dithiole rings are located such that no significant steric interactions occur. It is important to prevent steric congestion between contiguous monomer units.[10] Furthermore, the intramolecular short S···S contacts expected in **2** and **4** may be useful for the delocalization of electrons. We report here the preparation and properties of the monomers and their polymers.

[⊗] Abstract published in *Advance ACS Abstracts,* December 15, 1993.

(1) (a) Waltman, R. J.; Bargon, J. *Can. J. Chem.* **1986**, *64*, 76. (b) Skotheim, T. A., Ed. *Handbook of Conducting Polymers*; Marcel Dekker: New York, 1986. (c) Patil, A. O.; Heeger, A. J.; Wudl, F. *Chem. Rev.* **1988**, *88*, 183. (d) Ganier, F. *Angew. Chem., Int. Ed. Engl.* **1989**, *28*, 513. (e) Scherf, U.; Müllen, K. *Synthesis* **1992**, *1/2*, 23.

(2) Roncali, J. *Chem. Rev.* **1992**, *92*, 711.

(3) Yamamoto, T.; Sanechika, K.; Yamamoto, A. *Bull. Chem. Soc. Jpn.* **1983**, *56*, 1497. McCullough, R. D.; Lowe, R. D. *J. Chem. Soc., Chem. Commun.* **1992**, 70. Yamamoto, T.; Morita, A.; Miyazaki, Y.; Maruyama, T.; Wakayama, H.; Zhou, Z.-h.; Nakamura, Y.; Kanbara, T.; Sasaki, S.; Kubota, K. *Macromolecules* **1992**, *25*, 1214. Chen, T.-A.; Rieke, R. D. *J. Am. Chem. Soc.* **1992**, *114*, 10087. McCullough, R. D.; Lowe, R. D.; Jayaraman, M.; Anderson, D. L. *J. Org. Chem.* **1993**, *58*, 904. McCullough, R. D.; Tristram-Nagle, S.; Williams, S. P.; Lowe, R. D.; Jayaraman, M. *J. Am. Chem. Soc.* **1993**, *115*, 4910. Miyazaki, Y.; Kanbara, T.; Osakada, K.; Yamamoto, T. *Chem. Lett.* **1993**, 415.

(4) (a) Lazzaroni, R.; Taliani, C.; Zamboni, R.; Danieli, R.; Ostoja, P.; Porzio, W.; Brédas, J. L. *Synth. Met.* **1989**, *28*, C515. (b) Ikenoue, Y.; Wudl, F.; Heeger, A. J. *Synth. Met.* **1991**, *40*, 1. (c) Ferraris, J. P.; Lambert, T. L. *J. Chem. Soc., Chem. Commun.* **1991**, 1268. (d) Hieber, G.; Hanack, M.; Wurst, K.; Strähle, J. *Chem. Ber.* **1991**, *124*, 1597. (e) Pomerantz, M.; Chaloner-Gill, B.; Harding, L. O.; Tseng, J. J.; Pomerantz, W. J. *J. Chem. Soc., Chem. Commun.* **1992**, 1672. (f) Musmanni, S.; Ferraris, J. P. *J. Chem. Soc., Chem. Commun.* **1993**, 172. (g) Tanaka, S.; Yamashita, Y. *Synth. Met.* **1993**, *55*, 1251. (h) Hanack, M.; Schmid, U.; Röhrig, U.; Toussaint, J.-M.; Adant, C.; Brédas, J. L. *Chem. Ber.* **1993**, *126*, 1487.

(5) (a) Wudl, F.; Kobayashi, M.; Heeger, A. J. *J. Org. Chem.* **1984**, *49*, 3382. (b) Kobayashi, M.; Colaneri, N.; Boysel, M.; Wudl, F.; Heeger, A. J. *J. Chem. Phys.* **1985**, *82*, 5717.

(6) Williams, J. M.; Schultz, A. J.; Geiser, U.; Carlson, K. D.; Kini, A. M.; Wang, H. H.; Kwok, W.-K.; Whangbo, M.-H.; Schirber, J. E. *Science* **1991**, *252*, 1501. Yamashita, Y.; Tanaka, S.; Imaeda, K.; Inokuchi, H. *Chem. Lett.* **1991**, 1213. Bryce, M. R.; Cooke, G.; Dhindsa, A. S.; Ando, D. J.; Hursthouse, M. B. *Tetrahedron Lett.* **1992**, *33*, 1783.

(7) Taliani, C.; Ruani, G.; Zamboni, R.; Bolognesi, A.; Catellani, M.; Destri, S.; Porzio, W.; Ostoja, P. *Synth. Met.* **1989**, *28*, C507.

(8) Preliminary communication: Kozaki, M.; Tanaka, S.; Yamashita, Y. *J. Chem. Soc., Chem. Commun.* **1992**, 1137.

(9) Preliminary communication: Kozaki, M.; Tanaka, S.; Yamashita, Y. *Chem. Lett.* **1993**, 533.

(10) Schiavon, G.; Zotti, G.; Berlin, A.; Pagani, G.; Sannicolò, F. *Synth. Met.* **1989**, *28*, C199. Berlin, A.; Brenna, E.; Pagani, G. A.; Sannicolò, F.; Zotti, G.; Schiavon, G. *Synth. Met.* **1992**, *51*, 287.

0022-3263/94/1959-0442$04.50/0

Scheme 1[a]

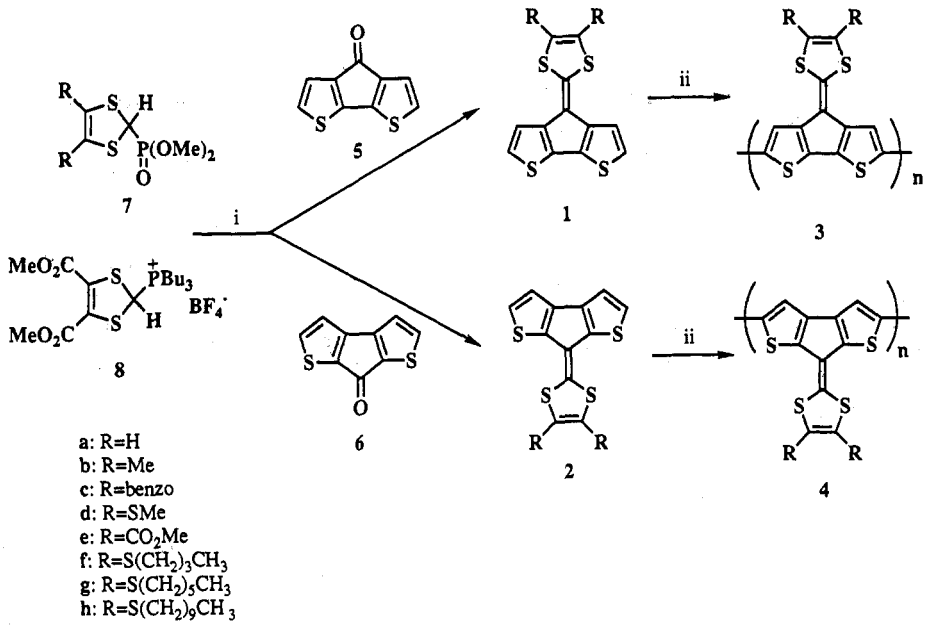

a: R=H
b: R=Me
c: R=benzo
d: R=SMe
e: R=CO_2Me
f: R=$S(CH_2)_3CH_3$
g: R=$S(CH_2)_5CH_3$
h: R=$S(CH_2)_9CH_3$

[a] Key: (i) *n*-BuLi/THF; (ii) electrolytic polymerization.

Table 1. Properties of 1,3-Dithiole Compounds 1 and 2

compd	R	yield/%	mp/°C	λ_{max}[a]/nm	E_{pa}/V vs SCE[b]
1a	H	65	171–173	411	0.87
1b	Me	71	223–224	419	0.83 (0.78)[c]
1c	benzo	89	212–213	400	0.92
1d	SMe	98	167–168	411	0.87
1e	CO_2Me	41	223–225	389	1.02
1f	$S(CH_2)_3CH_3$	78	71–72	412	0.88 (0.91)[c]
1g	$S(CH_2)_5CH_3$	96	oil	412	0.87 (0.97[c])
1h	$S(CH_2)_9CH_3$	64	54–56	412	0.86 (0.91[c])
2a	H	75	137	420	0.83
2b	Me	80	277	430	0.78
2c	benzo	80	215–217	414	0.97
2d	SMe	72	155–156	427	0.90
2e	CO_2Me	38	213–215	407	1.09

[a] Measured in EtOH (**1a–f**), *n*-hexane (**1g,h**), and CH_2Cl_2 (**2a–e**). [b] Measured by cyclic voltammetry in PhCN, 0.1 mol dm^{-3} TBAP, scan rate 100 mV s^{-1}, Pt electrode. [c] Measured in EtCN.

Results and Discussion

Preparation and Properties of the Monomers. Ketones **5** and **6**,[11] phosphonate esters **7**,[12] and the Wittig reagent **8**[13] were synthesized by reported methods. 1,3-Dithiole compounds **1a–d** were prepared in 64–95% yields by a Wittig–Horner reaction of **5** with carbanions derived from **7**. Similarly, compounds **2a–d** were prepared from the corresponding ketone **6** in 72–80% yields (Scheme 1). Dicarbomethoxy derivatives **1e** and **2e** were obtained by a Wittig reaction of **8** with **5** and **6** in 41 and 38% yields, respectively. Their properties are summarized in Table 1. Their absorption maxima are observed at longer wavelengths than that of TTF,[14] and introduction of electron donating groups makes the absorptions red-shifted, suggesting that some polarization exists in **1** and **2**.

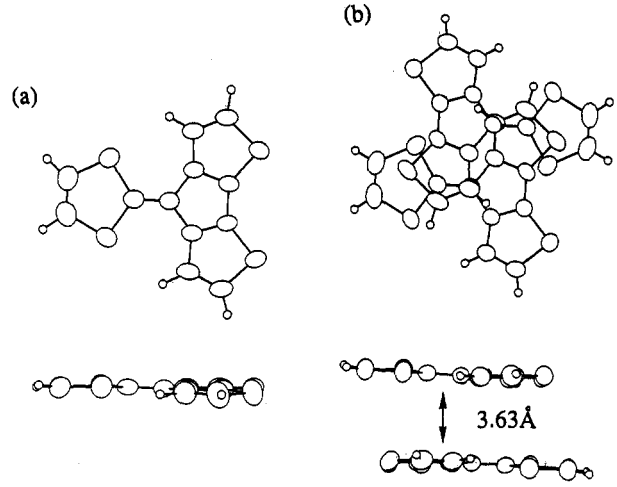

Figure 1. Molecular structure and overlap mode of **1a**: (a) molecule I, (b) molecule II.

The X-ray structural analysis of **1a** reveals that there are two crystallographically independent molecules (molecules I and II) which are almost planar (Figure 1). The crystal structure is shown in Figure 2, where three intermolecular S···S contacts (3.43, 3.43, and 3.51 Å), which are shorter than the sum of the van der Waals radii (3.70 Å), are observed between the thiophene rings of molecules II. In the crystal, molecules II are uniformly stacked along the *c* axis in a dimeric structure as shown in Figure 2. Distances between the molecular planes are 3.63 Å in the dimer and 3.97 Å between the dimers. On the other hand, the X-ray structural analysis of **2a** reveals that the molecule is almost planar and there are two intramolecular S···S contacts (3.39 and 3.38 Å) which are shorter than the sum of the van der Waals radii, as shown in Figure 3. Such short contacts may facilitate the delocalization of electrons. The crystal structure is shown in Figure 4, wherein a short intermolecular S···S contact (3.60 Å) is observed between the 1,3-dithiole rings. The molecules of **2a** are uniformly

(11) Jordens, P.; Rawson, G.; Wynberg, H. *J. Chem. Soc. C* **1970**, 273.
(12) Akiba, K.; Ishikawa, K.; Inamoto, N. *Bull. Chem. Soc. Jpn.* **1978**, *51*, 2674.
(13) Sato, M.; Gonnella, N. C.; Cava, M. P. *J. Org. Chem.* **1979**, *44*, 930.
(14) Wudl, F.; Smith, G. M.; Hufnagel, E. J. *J. Chem. Soc., Chem. Commun.* **1970**, 1453.

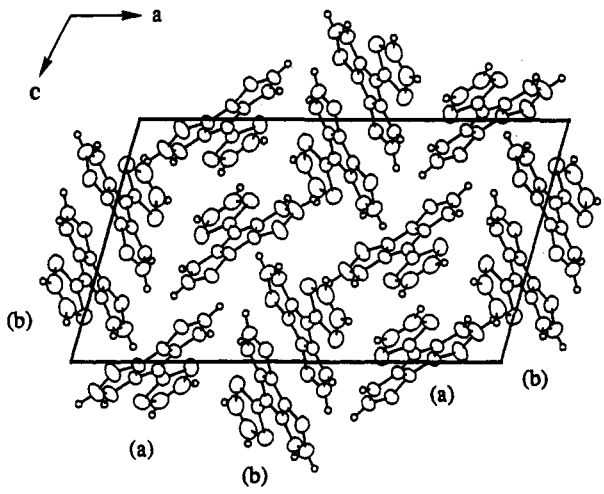

Figure 2. Crystal structure of **1a**: (a) molecule I, (b) molecule II.

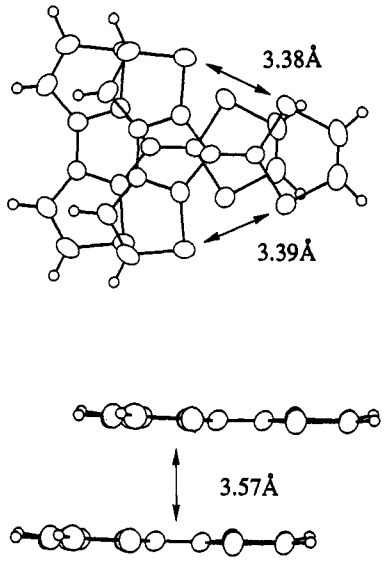

Figure 3. Molecular structure and overlap mode of **2a**.

stacked along the *b* axis with good overlap as shown in Figure 3. The distance between the molecular planes is 3.57 Å.

Cyclic voltammograms for **1a–e** and **2** were measured using a Pt disk as a working electrode, in PhCN containing 0.1 mol dm^{-3} tetrabutylammonium perchlorate (TBAP) as a supporting electrolyte, and with a scanning rate of 100 mV s^{-1}. They revealed irreversible oxidation waves (Figures 5 and 7). Their anodic peak potentials of these compounds (E_{pa}) are summarized in Table 1. The compounds **1** have E_{pa} values similar to the corresponding **2**. These values are significantly lower than that of bithiophene (1.44 V vs SCE).[15] This fact can be attributed to the electron-donating ability of the 1,3-dithiole rings. In both **1** and **2**, the E_{pa} are strongly dependent on the substituents, indicating that HOMOs in each molecule have large atomic orbital (AO) coefficients at the carbon atoms bearing the substituents. This shows that the electronic state can be easily modified by the introduction of substituents onto the 1,3-dithiole ring. Moreover, dicarbomethoxy derivatives **1e** and **2e** showed irreversible

(15) We measured the oxidation potentials of bithiophene and polythiophene under identical conditions.

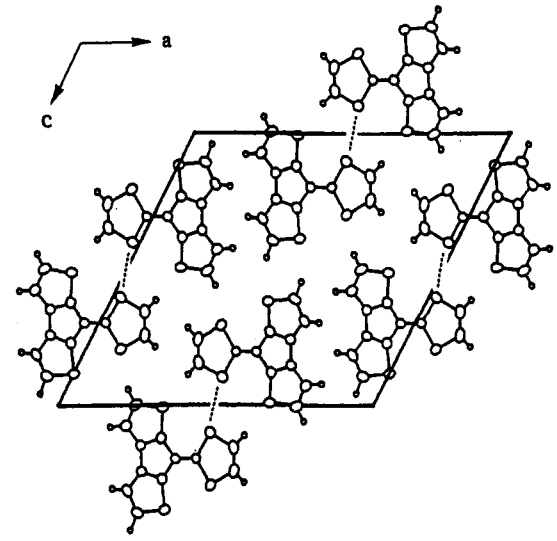

Figure 4. Crystal structure of **2a**: broken lines, S···S interactions [3.603(2) Å].

reduction waves with peak potentials (E_{pc}) of −1.32 V and −1.33 V vs SCE, respectively.

Preparation and Properties of Polymers. Polymers **3a,c–e** and **4** were prepared by the electrolytic oxidation of the corresponding monomers **1** and **2** using a Pt disk or indium–tin oxide (ITO) as a working electrode in 0.1 mol dm^{-3} TBAP/PhCN solution (Figures 5 and 7). For **3b**, EtCN was used as a solvent since PhCN yielded none. The peak current increased in the successive cycles, and a new peak appeared at lower potentials as shown in Figures 5 and 7, indicating the deposition and growth of polymers on the surface of the electrode. The E_{pa} values shifted gradually to higher potentials as the thickness of the polymer film increased. This is attributable to the IR drop across the film. The oxidation potentials of polymers **3a–e** and **4**, summarized in Table 2, were measured in monomer-free electrolytes. They are remarkably lower than that of polythiophene (1.03 V vs SCE).[15] Cyclic voltammograms of **3a** and **4a** measured at various scan rates are shown in Figures 6 and 8. They showed reversible peaks due to the p-doping. The anodic peak current (i_{pa}) in **3a** is proportional to the scan rate in the potential range of −1.0 to +1.0 V vs SCE as shown in Figure 6, indicating that the electrode reactions of the films are phenomenologically equivalent to that of a surface-attached redox species.[16] On the other hand, the dependence of the i_{pa} of **4a** on the scan rate is somewhere between linear and second order, in the potential range of −1.0 to +1.0 V vs SCE. After several repeated scans, the i_{pa} of **3a** was unchanged, but that of **4a** was slightly decreased, indicating that polymer **4a** is somewhat sensitive to the electrode potential.

The FT-IR spectra of the electrochemically dedoped film and doped films of **3** and **4** showed the characteristic peaks of monomers such as those around 1500 cm^{-1} due to the 1,3-dithiol-2-ylidene moiety (Table 7), indicating that the skeleton is intact in the polymers. On the other hand, a considerable decrease in the intensity of the peaks around 650 cm^{-1}, assigned to the C–H out-of-plane vibration, was observed after polymerization. The UV–

(16) Buttol, P.; Mastragostino, M.; Panero, S.; Scrosati, B. *Electrochim. Acta* **1986**, *31*, 783. Oyama, N.; Ohsaka, T.; Miyamoto, H. *Synth. Met.* **1989**, *28*, C193. Wei, Y.; Chan, C.-C.; Tian, J.; Jang, G.-W.; Hsueh, K. F. *Chem. Mater.* **1991**, *3*, 888.

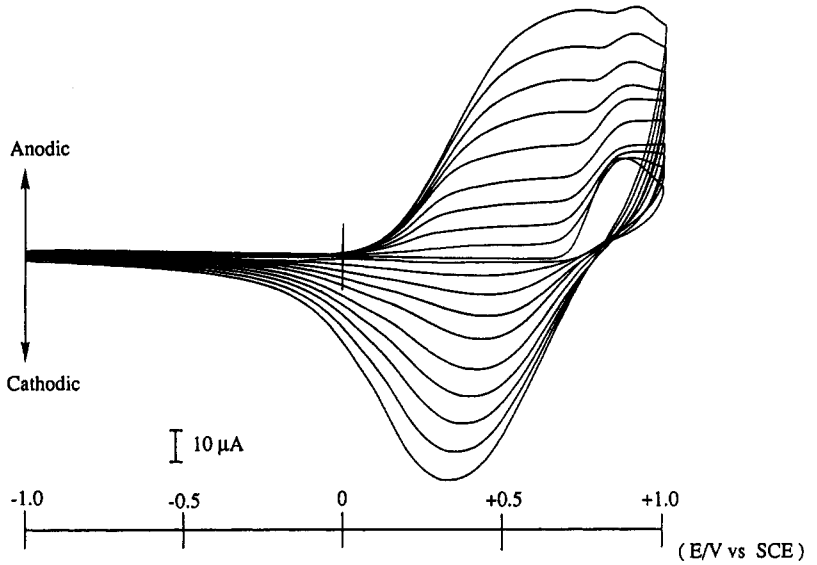

Figure 5. Successive cyclic voltammograms of **1a** in PhCN containing 0.1 mol dm^{-3} TBAP, scan rate 100 mV s^{-1}. They were recorded every five cycles. A platinum disk and SCE were used as a working and a reference electrode, respectively.

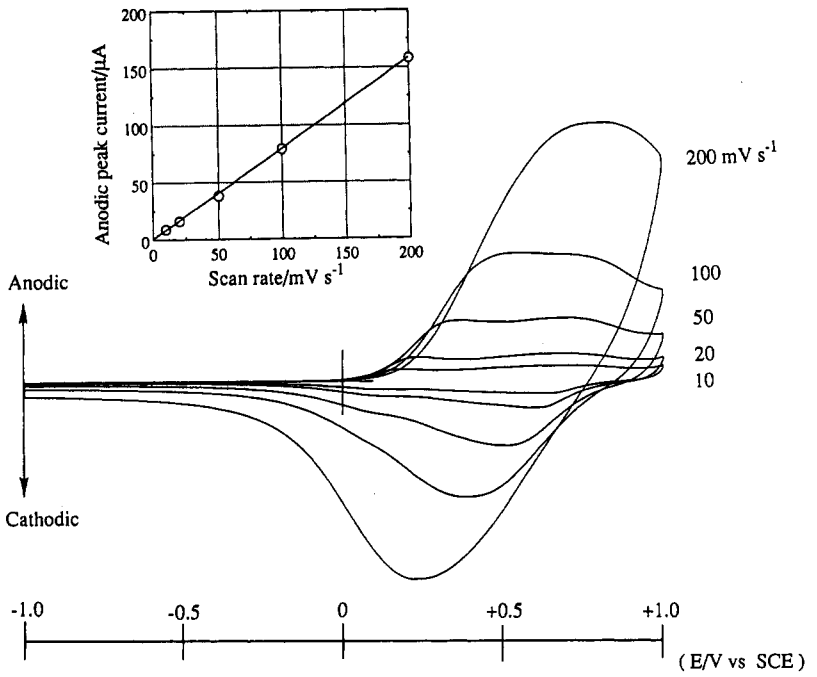

Figure 6. Cyclic voltammograms of **3a** measured in a monomer-free PhCN/0.1 mol dm^{-3} TBAP at various scan rates under an argon atmosphere. A platinum disk and SCE were used as a working and a reference electrode, respectively. The insert shows the dependence of i_{pa} on scan rate.

vis–NIR spectra of the electrochemically dedoped films on ITO showed peaks at λ_{max} = 614–689 nm for **3a–e** and 444–584 nm for **4** (Table 2), indicating that **3a–e** and **4** have extended conjugated systems. Additional absorptions in longer wavelength regions were observed in the doped films due to the formation of polarons and/or bipolarons. Electrochemical cycles between the doping and dedoping states were accompanied by reversible color changes (typically from green (dedoping) to blue (doping)).

In order to investigate a dependence of the conducting properties of the polymers on anions contained in the supporting electrolytes, polymerizations were carried out by the constant potential method using an ITO electrode in PhCN containing TBAP, tetrabutylammonium tetrafluoroborate ($TBABF_4$), tetrabutylammonium hexafluorophosphate ($TBAPF_6$), or tetraethylammonium *p*-toluenesulfonate (TEAOTs) as supporting electrolytes. The potentials for the polymerizations were set somewhat lower than the E_{pa} of the monomers. The conductivities of the films so grown were measured by a four- or two-probe method. The typical thicknesses of the films measured by a scanning electron microscope (SEM) were 1–30 μm. Some combinations of the monomers and anions shown in Table 3 gave free standing films tough enough for measurements of conductivities. It is notable that some films such as **3c**·$(PF_6^-)_x$, **3e**·$(ClO_4^-)_x$, and **3e**·$(BF_4^-)_x$ showed conductivities as high as the doped film of PITN (50 S cm^{-1}).[5b] The conductivities of other films such as **3a**·$(ClO_4^-)_x$, **3d**·$(ClO_4^-)_x$, and **4c**·$(PF_6^-)_x$ were also higher than those of heterocycle-fused polythiophenes such as poly(dithieno[3,2-*b*;2′,3′-*d*]thiophene) (0.4 S cm^{-1})[4a] and poly(2,3-dihexylthieno[3,4-*b*]pyrazine) (3×10^{-2} S cm^{-1}).[4e]

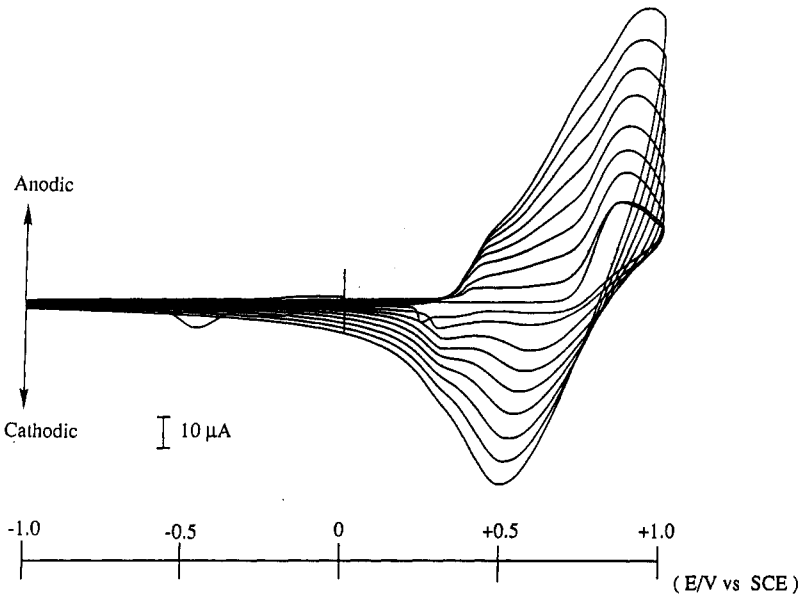

Figure 7. Successive cyclic voltammograms of **2a** in PhCN containing 0.1 mol dm^{-3} TBAP, scan rate 100 mV s^{-1}. They were recorded every five cycles. A platinum disk and SCE were used as a working and a reference electrode, respectively.

Table 2. Oxidation Potentials and Absorption Maxima of Polymers

polymer	R	E_{pa}/V vs SCE[a]	λ_{max}[b]/nm
3a	H	0.65	629
3b	Me	0.65	614
3c	benzo	0.70	626
3d	SMe	0.61	662
3e	CO_2Me	0.59	689
3f	$S(CH_2)_3CH_3$	0.62	660
3g	$S(CH_2)_5CH_3$	0.58	653
3h	$S(CH_2)_9CH_3$	0.56	650
4a	H	0.72	448
4b	Me	0.63	584
4c	benzo	0.76	562
4d	SMe	0.77	457
4e	CO_2Me	0.84	424

[a] Measured by cyclic voltammetry in PhCN for **3a**, **c–e**, and **4**, and EtCN for **3b**, **f–g**, 0.1 mol dm^{-3} TBAP, scan rate 10 mV s^{-1}, Pt electrode. [b] Measured on ITO.

The doping states of **3a–e** and **4** are stable, and the conductivities did not change after storage under air for a month. On the other hand, **3a**·$(OTs^-)_x$, **3a**·$(BF_4^-)_x$, and **4a**·$(OTs^-)_x$ gave physically strong films, but their conductivities were lower. Polymers **3a–e** generally have a tendency to give films with better conductivities than **4**. Most of the superficial morphologies of the films of **3a–e** and **4** observed by SEM show a granular appearance similar to that of polythiophene,[17] whereas **3a**·$(OTs^-)_x$ and **4a**·$(OTs^-)_x$ have very smooth, flat surfaces. Moreover, these films were very thick (20–30 μm).

For doped films of **3** and **4**, elemental analyses were performed to learn about the polymer structures and doping levels. At first, films so grown were washed with acetonitrile using a soxhlet with a glass filter to remove monomer and the supporting electrode. Then, washed films were dried at 60 °C in vacuo. Some films such as **3b**·$(ClO_4^-)_x$, **4a**·$(PF_6^-)_x$, and **4b**·$(BF_4^-)_x$, which were prepared as physically weak ones, became powder and passed through the glass filter during washing. Therefore, it was impossible to perform their elemental analyses. As described in the discussion about the conductivity measurements, polymers **4** tended to give very weak films. On the other hand, the polymers containing OTs^- were so hygroscopic that the elemental analyses could not be carried out. The results of elemental analyses are shown in Table 4. The doping levels estimated from the values of the analyses are reasonable compared with those of other polythiophene derivatives which show ca. 0.3 for a monomer unit.[1c,19a] Exceptions are **3c**·$(ClO_4^-)_x$ and **3c**·$(BF_4^-)_x$. These films showed significantly higher values than other poly(thiophenes) although the conductivities are comparable.

Preparation and Properties of Alkyl-Substituted Polymers. The introduction of linear alkyl chains into polymers increases their solubility in solvents and lends structural control.[18] With this in mind, compounds **1f–h**, containing linear alkyl chains, were synthesized in 64–96% yields using a method similar to that described above. In **1f–h**, introduction of linear alkyl chains dramatically lowered their melting points, and in particular, that of **1g** was below room temperature (Table 1). On the other hand, the alkyl chain length had no effect on the electronic spectrum and E_{pa}. Electrochemical polymerizations performed under the conditions described above, except for varying solvent, gave the corresponding polymers **3f–h**. For electrochemical polymerizations of **1f–h**, EtCN was used as solvent since no polymer formed in PhCN. This can be explained by the notion that reaction intermediates that would otherwise lead to polymers dissolved in PhCN and thus diffused away from the electrode surface. This is supported by the observation that, during the polymerizations, the color of the solution around the surface of the electrode changed to green. After polymerization, the films were washed with EtCN to remove the supporting electrolytes and the monomers. Although **3f–h** were

(17) Waltman, R. J.; Bargon, J.; Diaz, A. F. *J. Phys. Chem.* **1983**, *87*, 1459.

(18) Sato, M.; Tanaka, S.; Kaeriyama, K. *J. Chem. Soc., Chem. Commun.* **1986**, 873. Jen, K.-Y.; Miller, G. G.; Elsenbaumer, R. L. *J. Chem. Soc., Chem. Commun.* **1986**, 1346. Bryce, M. R.; Chissel, A.; Kathirgamanathan, P.; Parker, D.; Smith, N. R. M. *J. Chem. Soc., Chem. Commun.* **1987**, 466. Hotta, S.; Rughooputh, S. D. D. V.; Heeger, A. J.; Wudl, F. *Macromolecules* **1987**, *20*, 212. Roncali, J.; Garreau, R.; Yassar, A.; Marque, P.; Garnier, F.; Lemaire, M. *J. Phys. Chem.* **1987**, *91*, 6706. Kawai, T.; Kuwabara, T.; Wang, S.; Yoshino, K. *J. Electrochem. Soc.* **1990**, *137*, 3793.

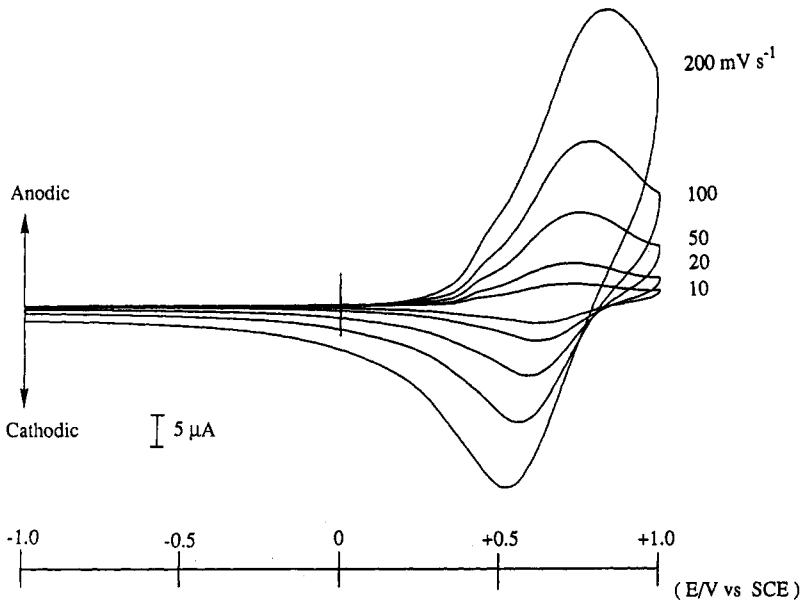

Figure 8. Cyclic voltammograms of **4a** measured in a monomer-free PhCN/0.1 mol dm^{-3} TBAP at various scan rates under an argon atmosphere. A platinum disk and SCE were used as a working and a reference electrode, respectively.

Table 3. Conductivities of Oxidized Polymers

polymer	R	X	potential/ V vs SCE[a]	σ^b/S cm^{-1}
3a	H	ClO_4^-	0.70	4.1×10^{-1}
		BF_4^-	1.10	1.1×10^{-3}
		OTs^-	0.70	2.7×10^{-3}
3b	Me	ClO_4^-	0.75	4.4×10^{-1}
3c	benzo	ClO_4^-	0.75	4.4×10^{-1}
		BF_4^-	1.20	3.2×10^{-1}
		PF_6^-	0.85	33
		OTs^-	0.90	3.3×10^{-1}
3d	SMe	ClO_4^-	0.70	1.7
3e	CO_2Me	ClO_4^-	0.85	41
		BF_4^-	1.20	52
		PF_6^-	0.90	46
3f	$S(CH_2)_3CH_3$	ClO_4^-	0.80	1.5×10^{-4c}
3g	$S(CH_2)_5CH_3$	ClO_4^-	0.80	3.7×10^{-4c}
3h	$S(CH_2)_9CH_3$	ClO_4^-	0.80	3.5×10^{-4c}
4a	H	ClO_4^-	0.75	2.5×10^{-2d}
		BF_4^-	0.85	2.0×10^{-3d}
		OTs^-	0.70	5.9×10^{-3}
4b	Me	ClO_4^-	0.80	3.0×10^{-3d}
		BF_4^-	0.80	5.8×10^{-4d}
		OTs^-	0.75	$<10^{-6d}$
4c	benzo	ClO_4^-	0.90	2.0×10^{-2}
		PF_6^-	0.85	2.0×10^{-1}
		OTs^-	0.95	1.9×10^{-3d}
4d	SMe	ClO_4^-	0.90	1.0×10^{-3d}

[a] Potentials for polymer syntheses. See Experimental Section. [b] Measured by a four-probe method. [c] Measured on compressed pellets by a two-probe method. [d] Measured by a two-probe method.

obtained as good free standing films, the structures of these films were like sponge and the thicknesses of the films could not be estimated. Thus, the electrical conductivities were measured on compressed pellets by a two-probe method (Table 3). The values were 3 or 4 orders of magnitude lower than those of other films of **3**. In the FT-IR spectra of electrochemically dedoped **3f–h**, absorption bands corresponding to the C–H vibrations of the alkyl groups were observed around 2950 cm^{-1} (Table 7). Both the electrochemically dedoped and doped films were partially soluble in organic solvents such as THF, chloroform, and carbon disulfide. The solubilities of the dedoped polymers were generally higher than those of the doped ones. Dedoped **3g** showed the best solubility, although there was still an insoluble component which

Table 4. Data for Elemental Analyses

polymer	X	molecular formula	analysis[a]
3a	ClO_4^-	$(C_{12}H_4S_4)(ClO_4^-)_{0.31}$	calcd C, 46.97; H, 1.31
			found C, 46.90; H, 1.70
	BF_4^-	$(C_{12}H_4S_4)(BF_4^-)_{0.17}$	calcd C, 49.50; H, 1.39
			found C, 49.65; H, 1.98
3c	ClO_4^-	$(C_{16}H_6S_4)(ClO_4^-)_{0.43}$	calcd C, 52.05; H, 1.64
			found C, 51.98; H, 2.05
	BF_4^-	$(C_{16}H_6S_4)(BF_4^-)_{0.46}$	calcd C, 52.45; H, 1.65
			found C, 52.45; H, 2.11
	PF_6^-	$(C_{16}H_6S_4)(PF_6^-)_{0.24}$	calcd C, 53.20; H, 1.67
			found C, 53.30; H, 2.17
3e	ClO_4^-	$(C_{16}H_8O_4S_4)(ClO_4^-)_{0.28}$	calcd C, 45.75; H, 1.92
			found C, 45.76; H, 2.07
	PF_6^-	$(C_{16}H_8O_4S_4)(PF_6^-)_{0.18}$	calcd C, 45.91; H, 1.93
			found C, 46.19; H, 2.07

[a] Inclusion of nitrogen on all samples was 0.00%.

probably consists of a higher molecular weight polymer. The soluble portion of **3g** was treated with hydrazine hydrate to give completely dedoped films and used for measurements of the ^{1}H NMR and electronic spectra. The ^{1}H NMR spectrum of **3g** showed some broad peaks, assigned to the hexyl protons, which appear at the same chemical shifts as those of **1g**. However, the peaks of the ring protons were not clearly discernible because of their broad signals. The electronic spectrum of **3g** in $CHCl_3$ showed an absorption maximum at 626 nm which is red-shifted by 27 nm relative to that of the film on ITO. This spectrum showed a clear base line and an absorption edge, as shown in Figure 9. This fact indicates that charges still remain in the electrochemically dedoped films. The bandgap of **3g**, estimated from the absorption edge, is around 1.4 eV which is much narrower than that of polythiophene (2.1 eV).[19] The GPC analysis of **3g** in THF indicated a weight-average molecular weight (M_w) of 5456 (polystyrene standard) with a polydispersity of 2.0, which corresponds to about 11 monomer units.

Molecular Orbital Calculation Results. MNDO-PM3 calculations[20] show that **1a** has very large AO

(19) (a) Chung, T.-C.; Kaufman, J. H.; Heeger, A. J.; Wudl, F. *Phys. Rev. B* **1984**, *30*, 702. (b) Taliani, C.; Danieli, R.; Zamboni, R.; Ostoja, P.; Porzio *Synth. Met.* **1987**, *18*, 177.

(20) Stewart, J. J. P. *J. Comput. Chem.* **1989**, *10*, 209, 221.

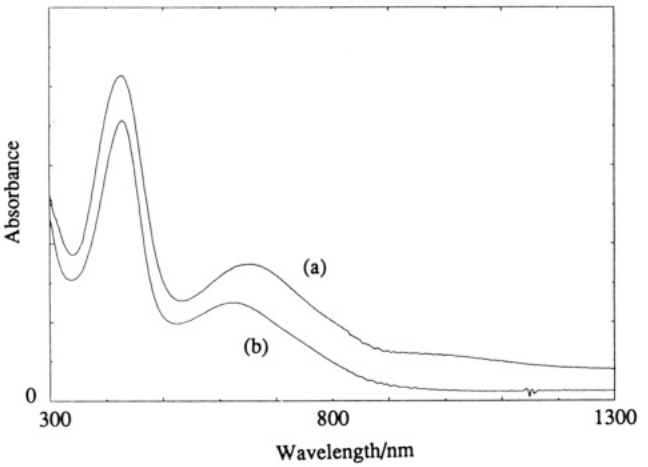

Figure 9. Absorption spectra of (a) electrochemically dedoped thin film of **3g** on ITO and (b) hydrazine-treated **3g** in $CHCl_3$.

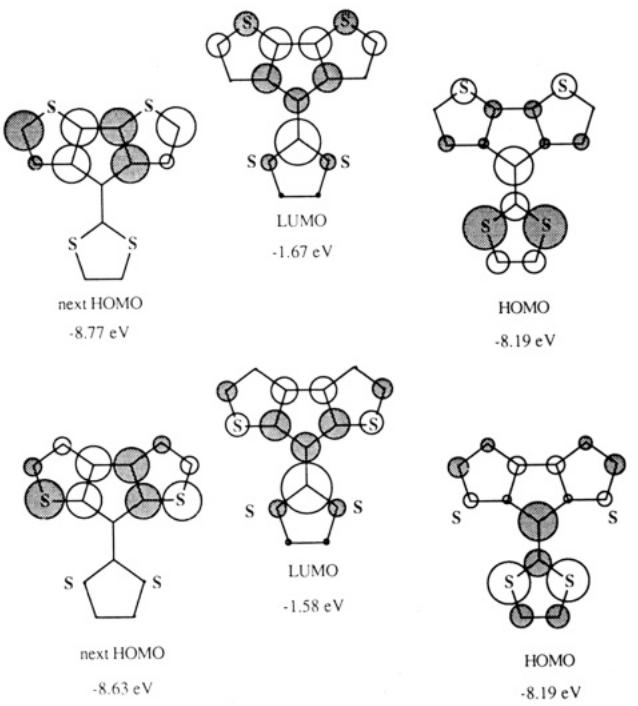

Figure 10. AO coefficients in next HOMOs, HOMOs, and LUMOs of **1a** (upper) and **2a** (lower) calculated by the MNDO-PM3 method. The radii of circles are approximately proportional to the magnitude of the coefficients.

coefficients at the carbon atoms at the α-positions of the thiophene rings in the next-HOMO, while the AO coefficients at the α- and β-carbon atoms at the thiophene rings are smaller in the HOMO as shown in Figure 10. On the other hand, **2a** has larger AO coefficients at the α-positions than at the β-positions in the HOMO. These facts suggest that the electropolymerizations proceed predominantly at the α-positions. The HOMOs of **1a** and **2a** also have large AO coefficients at the 3- and 4-positions of the 1,3-dithiole ring. This fact is consistent with the observation that the electronic properties of **1** and **2** were greatly affected by the introduction of substituents at these positions.

The difference in the absorption spectra of **3** and **4** (Table 2) indicates that more delocalization of π-electrons takes place in **3** than in **4**. This may be attributable to the torsion between the monomer units. We have investigated this possibility with MO calculations.[1a,21] First, to obtain information about the energy barrier for rotation around the interring C–C single bonds, reaction path calculations for this rotation were performed on the dimers derived from **1a** and **2a**. The calculations were carried out every 10° from 0° to 180° with optimization and showed very shallow energy minima at dihedral angles of about 30° (S–C–C–S) for both dimers, where the energy barrier heights are 0.89 and 0.83 kcal mol^{-1}, respectively. On the other hand, the calculations on bithiophene indicated a shallow potential minimum at 30° with an energy barrier height of 0.65 kcal mol^{-1}. These results suggest that polymers **3a** and **4a** have steric interactions between the monomer units that are comparable to those in polythiophene. Since terthiophene has a coplaner conformation in the crystal,[22] these results suggest that **3a** and **4a** also have coplanar conformations in the solid state.

Table 5. Absorption Maxima of the Oligomers Derived from 1a and 2a Calculated by the INDO/1 method

compd		λ_{max}/nm (log ϵ)	$\Delta\lambda_{max}$[a]
1a	monomer	510 (3.92)	
	dimer	594 (4.58)	84
	trimer	647 (4.80)	137
	tetramer	671 (4.95)	161
2a	monomer	361 (4.54)[b]	
	dimer	475 (4.03)	114
	trimer	482 (4.26)	121
	tetramer	484 (4.46)	123
	bithiophene	323 (4.63)	

[a] $\Delta\lambda_{max} = \lambda_{max}$(monomer) – λ_{max}(oligomer). [b] There is a forbidden transition at 447 nm.

Absorption maxima of the structure-optimized oligomers shown in Table 5 were calculated by the INDO/1 method using Zener's parameters.[23] We performed the configuration interaction (CI) calculations up to 100 configuration functions. The calculations show that the oligomers derived from **1a** have absorptions with larger molar decadic absorption coefficients (ϵ) at longer wavelengths than those derived from **2a**. In addition, as the oligomerization proceeds, the absorption maxima are more blue-shifted in **1a** than in **2a**. These results are in agreement with the physical observations and indicate that the difference in the absorption maxima of **3a** and **4a** can be attributed to the intrinsic electronic character of each molecule.

Conclusion

Two types of novel polythiophene derivatives containing 1,3-dithiole moieties were electrochemically prepared. The polymers showing low oxidation potentials were very stable. Some polymers exhibited high conductivities which can be attributed to the 1,3-dithiole groups. The polymers **3** showed higher conductivities than isomers **4**. Investigation of the properties of the monomers revealed that the introduction of 1,3-dithiole groups leads to an increase in the intermolecular interactions, stability of radical cations, and polarization of molecules. The polymers **3** have smaller bandgaps than **4** as observed in

(21) Samdal, S.; Samuelsen, E. J.; Volden, H. V. *Synth. Met.* **1993**, *59*, 259.
(22) Bolhuis, F. V.; Wynberg, H.; Havinga, E. E.; Meijer, E. W.; Staring, E. G. J. *Synth. Met.* **1989**, *30*, 381.
(23) Ridley, J. E.; Zerner, M. C. *Theor. Chim. Acta* **1973**, *32*, 111. Bacon, A. D.; Zerner, M. C. *Theor. Chim. Acta* **1979**, *53*, 21. Zerner, M. C.; Loew, G. H.; Kirchner, R. F.; Mueller-Westerhoff, U. T. *J. Am. Chem. Soc.* **1980**, *102*, 589.

their absorption spectra. This result was explained by differences in the conjugation across the monomer units, which were investigated by MO calculations. Effective conjugation across monomer units proves to be important. MO calculations also indicated little steric hindrance between the monomer units, in both polymers. Finally, the introduction of long alkyl chains improved the solubility of the polymers, and simple methods for the preparation of 1,3-dithiole derivatives made these modifications simple.

Experimental Section

General. Melting points are uncorrected. Infrared spectra were taken in KBr pellets. Mass spectra were obtained in the EI mode at 70 eV unless indicated otherwise.

General Procedure for Wittig–Horner and Wittig Reactions. To the carbanions prepared from 7 or 8 (2.0–4.0 mmol) and *n*-BuLi in hexane (1.8–3.6 mmol) in dry THF (10 mL) at −78 °C under argon was added 5 or 6 (1.0 mmol). This solution was stirred for 15 min at −78 °C. After a cooling bath was removed, the solution was further stirred for 20 min. The solvent was evaporated in vacuo. The resulting residue was diluted with water and extracted with CH_2Cl_2. The solution was washed with brine and water and dried over anhydrous $MgSO_4$. After evaporation of the solvent, the resulting solid was purified by recrystallization.

1a: orange crystals, mp 171–173 °C (from CCl_4); ^1H NMR ($CDCl_3$) δ 6.66 (s, 2 H), 7.14 (d, J = 5.0 Hz, 2 H), 7.21 (d, J = 5.0 Hz, 2 H); IR (KBr) 1567, 1520, 1373, 831, 652 cm^{-1}; UV (EtOH) λ_{max} 264 nm (log ϵ 4.33), 397 (4.39, sh), 411 (4.45); MS m/z (relative intensity) 278 (M^+, 100), 220 (23), 176 (12). Anal. Calcd for $C_{12}H_6S_4$: C, 51.81; H, 2.18. Found: C, 51.67; H, 2.33.

1b: yellow crystals, mp 223–224 °C (from EtOAc); ^1H NMR ($CDCl_3$) δ 2.07 (s, 6 H), 7.11 (d, J = 4.9 Hz, 2 H), 7.18 (d, J = 4.9 Hz, 2 H); IR (KBr) 1540, 1374, 828, 659 cm^{-1}; UV (EtOH) λ_{max} 265 nm (log ϵ 4.20), 403 (4.26, sh), 408 (4.33); MS m/z (relative intensity) 306 (M^+, 100), 220 (9), 176 (8). Anal. Calcd for $C_{14}H_{10}S_4$: C, 54.91; H, 3.29. Found: C, 54.81; H, 3.37.

1c: orange crystals, mp 212–213 °C (from $CHCl_3$); ^1H NMR ($CDCl_3$) δ 7.15 (d, J = 4.9 Hz, 2 H), 7.23 (dd, J = 3.2, 6.0 Hz, 2 H), 7.29 (d, J = 4.9 Hz, 2 H), 7.42 (dd, J = 3.2, 6.0 Hz, 2 H); IR (KBr) 1575, 1553, 830, 672 cm^{-1}; UV (EtOH) λ_{max} 252 nm (log ϵ 4.36), 263 (4.38), 382 (4.46), 400 (4.52); MS m/z (relative intensity) 328 (M^+, 100), 296 (11), 164 (16). Anal. Calcd for $C_{16}H_8S_4$: C, 58.55; H, 2.46. Found: C, 58.26; H, 2.49.

1d: orange crystals, mp 167–168 °C (from acetone); ^1H NMR ($CDCl_3$) δ 2.52 (s, 6 H), 7.13 (d, J = 4.9 Hz, 2 H), 7.15 (d, J = 4.9 Hz, 2 H); IR (KBr) 1560, 1488, 1368, 670 cm^{-1}; UV (EtOH) λ_{max} 266 nm (log ϵ 4.56), 411 (4.61); MS m/z (relative intensity) 370 (M^+, 100), 322 (36), 220 (88). Anal. Calcd for $C_{14}H_{10}S_6$: C, 45.42; H, 2.72. Found: C, 45.22; H, 2.68.

1e: orange crystals, mp 223–225 °C (from EtOAc); ^1H NMR ($CDCl_3$) δ 3.92 (s, 6 H), 7.14 (s, 4 H); (C_6D_6) δ 3.29 (s, 6 H), 6.64 (d, J = 5.0 Hz, 2 H), 6.88 (d, J = 5.0 Hz, 2 H); IR (KBr) 1750, 1709, 1579, 1272, 1236, 661 cm^{-1}; UV (EtOH) λ_{max} 263 nm (log ϵ 4.21), 389 (4.29); MS m/z (relative intensity) 394 (M^+, 100), 220 (39), 176 (12). Anal. Calcd for $C_{16}H_{10}O_4S_4$: C, 48.74; H, 2.56. Found: C, 48.59; H, 2.74.

1f: orange crystals, mp 71–72 °C (from EtOH); ^1H NMR ($CDCl_3$) δ 0.95 (t, J = 7.5 Hz, 6 H), 1.48 (m, 4 H), 1.68 (tt, J = 7.3, 7.3 Hz, 4 H), 2.92 (t, J = 7.3 Hz, 4 H), 7.13 (d, J = 5.2 Hz, 2 H), 7.16 (d, J = 5.2 Hz, 2 H); IR (KBr) 2956, 1561, 1374, 660 cm^{-1}; UV (EtOH) λ_{max} 266 nm (log ϵ 4.33), 412 (4.44); MS m/z (relative intensity) 454 (M^+, 100), 364 (42), 341 (20), 220 (56). Anal. Calcd for $C_{20}H_{22}S_6$: C, 52.86; H, 4.88. Found: C, 53.02; H, 5.03.

1g: orange oil; ^1H NMR ($CDCl_3$) δ 0.90 (t, J = 6.9 Hz, 6 H), 1.31 (m, 8 H), 1.45 (m, 4 H), 1.69 (tt, J = 7.4, 7.5 Hz, 4 H), 2.90 (t, J = 7.4 Hz, 4 H), 7.13 (d, J = 5.0 Hz, 2 H), 7.16 (d, J = 5.0 Hz, 2 H); IR (NaCl) 2922, 1678, 1565, 1371 cm^{-1}; UV (Hexane) λ_{max} 266 nm (log ϵ 4.31), 396 (4.38), 411 (4.46); MS m/z (relative intensity) 510 (M^+, 100), 392 (21), 341 (13), 220 (27). Anal. Calcd for $C_{24}H_{30}S_6$: C, 56.46; H, 5.93. Found: C, 56.05; H, 5.79.

Table 6. Crystal Data for 1,3-Dithiole Compounds 1a and 2a

compd	1a	2a
formula	$C_{12}H_6S_4$	$C_{12}H_6S_4$
f_w	278.42	278.42
space group	$P2_1/n$	$P2_1/n$
a (Å)	21.093(18)	18.297(5)
b (Å)	9.404(1)	4.006(0)
c (Å)	12.185(1)	17.220(0)
α (deg)	90.0	90.0
β (deg)	105.95(1)	118.05(1)
λ(deg)	90.0	90.0
V (Å^3)	2315.9(4)	1113.9(4)
Z	8	4
ρ_{calcd} (g cm^{-3})	1.60	1.96
cryst size (mm)	0.05 × 0.11 × 0.34	0.13 × 0.18 × 0.49
radiation	Cu Kα	Cu Kα
$2\theta_{max}$ (deg)	1, 70	1, 70
total data measd	4403	2458
obsd unique data	3794 (3σ)	1897 (3σ)
R	0.0673	0.0776

1h: yellow crystals, mp 54–56 °C (from EtOH); ^1H NMR ($CDCl_3$) δ 0.87 (t, J = 6.9 Hz, 6 H), 1.29 (m, 24 H), 1.44 (m, 4 H), 1.69 (tt, J = 7.4, 7.4 Hz, 4 H), 2.91 (t, J = 7.4 Hz, 4 H), 7.13 (d, J = 5.0 Hz, 2 H), 7.16 (d, J = 5.0 Hz, 2 H); IR (KBr) 2922, 1561, 1373, 670 cm^{-1}; UV (hexane) λ_{max} 266 nm (log ϵ 4.36), 396 (4.44), 411 (4.53); MS m/z (relative intensity) 622 (M^+, 100), 488 (16), 341 (17), 220 (48). Anal. Calcd for $C_{32}H_{46}S_6$: C, 61.72; H, 7.45. Found: C, 61.74; H, 7.28.

2a: yellow crystals, mp 143–144 °C (from benzene); ^1H NMR ($CDCl_3$) δ 6.81 (s, 2 H), 7.21 (d, J = 4.9 Hz, 2 H), 7.35 (d, J = 4.9 Hz, 2 H); IR (KBr) 1569, 705, 641 cm^{-1}; UV (CH_2Cl_2) λ_{max} 253 nm (log ϵ 4.26), 281 (4.04), 405 (4.33), 420 (4.37); MS m/z (relative intensity) 278 (M^+, 100), 220 (18), 176 (14). Anal. Calcd for $C_{12}H_6S_4$: C, 51.81; H, 2.18. Found: C, 51.60; H, 2.37.

2b: yellow crystals, mp 277 °C (from EtOAc); ^1H NMR ($CDCl_3$) δ 2.16 (s, 6 H), 7.20 (d, J = 4.9 Hz, 2 H), 7.32 (d, J = 4.9 Hz, 2 H); IR (KBr) 1543, 1507, 708, 641 cm^{-1}; UV (CH_2Cl_2) λ_{max} 253 nm (log ϵ 4.26), 281 (4.04), 405 (4.33), 420 (4.37); MS m/z (relative intensity) 306 (M^+, 100), 220 (18), 176 (19). Anal. Calcd for $C_{14}H_{10}S_4$: C, 54.90; H, 3.28. Found: C, 54.97; H, 3.48.

2c: yellow crystals, mp 215–217 °C (from EtOAc); ^1H NMR ($CDCl_3$) δ 7.20 (d, J = 4.9 Hz, 2 H), 7.29 (dd, J = 3.2, 6.0 Hz, 2 H), 7.38 (d, J = 4.9 Hz, 2 H), 7.53 (dd, J = 3.2, 6.0 Hz, 2 H); IR (KBr) 1576, 1554, 744, 709, 646 cm^{-1}; UV (CH_2Cl_2) λ_{max} 252 nm (log ϵ 4.41), 276 (4.11, sh), 309 (3.56, sh), 402 (4.46, sh), 414 (4.50); MS m/z (relative intensity) 328 (M^+, 100), 164 (9), 93 (12). Anal. Calcd for $C_{12}H_6S_4$: C, 58.55; H, 2.46. Found: C, 58.35; H, 2.45.

2d: yellow crystals, mp 155–156 °C (from EtOAc); ^1H NMR ($CDCl_3$) δ 2.56 (s, 6 H), 7.19 (d, J = 4.7 Hz, 2 H), 7.35 (d, J = 4.7 Hz, 2 H); IR (KBr) 1560, 1484, 712 cm^{-1}; UV (CH_2Cl_2) λ_{max} 253 nm (log ϵ 4.26), 281 (4.04), 405 (4.33), 420 (4.37); MS m/z (relative intensity) 370 (M^+, 88), 220 (100), 176 (32). Anal. Calcd for $C_{14}H_{10}S_6$: C, 45.42; H, 2.72. Found: C, 45.39; H, 2.89.

2e: yellow crystals, mp 226 °C (from EtOAc); ^1H NMR ($CDCl_3$) δ 3.94 (s, 6 H), 7.17 (d, J = 4.9 Hz, 2 H), 7.38 (d, J = 4.9 Hz, 2 H); IR (KBr) 1744, 1726, 1585, 1248, 721, 650 cm^{-1}; UV (CH_2Cl_2) λ_{max} 253 nm (log ϵ 4.26), 281 (4.04), 405 (4.33), 420 (4.37); MS m/z (relative intensity) 394 (M^+, 100), 220 (48), 176 (15). Anal. Calcd for $C_{16}H_{10}O_4S_4$: C, 48.74; H, 2.56. Found: C, 48.89; H, 2.62.

X-ray Structural Analyses. The crystals for the data collections were prepared by slow evaporation of the solvents used for recrystallizations. An Enraf-Nonius CAD4 diffractometor was used with graphite-monochromated Cu Kα radiation; $\theta/2\theta$ scan technique. The crystal data are summarized in Table 6. Cell parameters were determined from least-squares procedures on 25 reflections (44° < 2θ < 50°). No significant variation was observed in intensities of three standards monitored every 7200 s. The structures were solved by the direct method using the MULTAN78 program[24] and refined by the block-diagonal

(24) Main, P.; Hull, S. E.; Lessinger, L.; Germain, G.; Declercq, J.-P.; Woolfson, M. M. MULTAN78, A system of Computer Programs for the Automatic Solution of Crystal Structures from X-ray Diffraction Data, Universities of York, England and Louvain, Belgium, 1978.

least-squares analysis based on F values using UNICS III program package.[25] All the non-hydrogen atoms of the molecule were refined with anisotropic temperature factors. The positions of hydrogen atoms were determined by a difference Fourier synthesis. At the final stage, hydrogen atoms were included in the refinement with isotropic temperature factors. These calculations were carried out in the Computer Center of Institute for Molecular Science.[27]

Electrochemical Measurements. All cyclic voltammetries were carried out with a three-component cell in distilled PhCN or EtCN containing 0.1 mol dm^{-3} TBAP at scan rate of 100 mV s^{-1}. The solution was degassed by argon bubbling before an electrochemical measurement which was performed under an argon atmosphere. A Pt disk, Pt wire, and SCE electrode were used as a working, counter, and reference electrode, respectively.

The polymers for cyclic voltammetries were prepared by a cyclic potential-sweep technique using the above conditions. The resulting polymers on the electrode were thoroughly washed with PhCN or EtCN. Cyclic voltammograms of the polymers were then recorded in monomer-free electrolytes under the same conditions as above except for a scan rate. In order to avoid shifts of the E_{pa} arising from the IR drop across the films, cyclic voltammograms of the polymers were measured at a scan rate of 10 mV s^{-1}.

General Procedure for Electrochemical Polymerizations. The polymers for the conductivity measurements were prepared by a constant potential method using an ITO, Pt wire, and SCE as a working, counter, reference electrode, respectively, in distilled PhCN (EtCN for **3b**) containing 0.01–0.03 mol dm^{-3} monomer and 0.1 mol dm^{-3} supporting electrolytes. The potentials are shown in Table 3. After degassing by argon, the polymerizations were performed under argon until a current became slight. The films so grown were peeled off from the electrode in MeCN, rinsed with MeCN, and dried. The polymers were yielded as black films. The conductivity measurements were carried out by a four- or two-probe method. The thicknesses of the films were measured by SEM which was also used for the observation of a superficial morphology of the films.

The polymers for elemental analyses were prepared by a constant potential technique under the same conditions as above. After the polymerizations, the resulting films were peeled off from ITO and thoroughly washed with MeCN. The films were further washed with MeCN using a soxhlet with a glass filter for 24 h and dried under vacuum at 60 °C for 24 h. Elemental analyses were performed twice for each sample to check homogeneities, and these two values agreed within 0.30%. Inclusion of nitrogen on all these samples was 0.00%.

The polymers for the measurements of absorption spectra were prepared by a cyclic potential-sweep technique under the conditions as described above except for using 2.0–6.0 mmol dm^{-3} monomer solutions. After the polymerizations, the resulting dark green films were thoroughly washed with PhCN (EtCN for **3b**). Then, electrochemical dedopings were carried out in monomer-free electrolytes at the most negative potentials which do no serious damage to the films and ITO. Before the measurements of electronic spectra, the dedoped films were rinsed with MeCN.

(25) Sakurai, T.; Kobayashi, K. *Rikagaku Kenkyusho Hokoku*, **1979**, *55*, 69.

Table 7. Spectroscopic Properties of Electrochemically Dedoped Polymers

polymer	IR/cm^{-1}	UV–vis/nm
3a	1555, 1515, 1286, 1210, 662	422, 629
3b	1532, 1437, 1265, 1122, 668	323, 433, 614
3c	1572, 1546, 1202, 1102, 666	413, 626
3d	1553, 1485, 1414, 1269, 968	317, 436, 662
3e	1714, 1567, 1433, 1252, 728	324, 423, 689
3f	2953, 1553, 1269, 1208, 728	432, 660
3g	2923, 1557, 1374, 1281, 720	425, 653
3h	2922, 1557, 1414, 1280, 721	429, 650
4a	1552, 1423, 1261, 1074, 834	326, 448
4b	1542, 1420, 1263, 1081, 836	378, 584
4c	1573, 1552, 1122, 834, 739	432, 562
4d	1540, 1429, 1264, 1075, 836	359, 457
4e	1734, 1579, 1433, 1260, 835	316, 424

On the other hand, for FT-IR measurements the dedoped films were peeled off from ITO, washed with MeCN, and dried. Spectroscopic properties of the electrochemically dedoped polymers are displayed in Table 7.

In the case of **3f–h**, the electrochemically dedoped films prepared in EtCN were washed with EtCN and then dissolved in $CHCl_3$. After filtration, the filtrates were further treated with a hydrazine solution. The solutions were washed with water and dried. After evaporation, dark green solids were obtained. The solid of **3g** was used for the measurement of electronic and ^1H NMR spectrum without a further treatment. ^1H NMR ($CDCl_3$) δ 0.88, 1.26, 1.58, 2.97; UV ($CHCl_3$) λ_{max} (relative intensity) 626 nm (100), 428 (40). For GPC analysis the solid of **3g** was washed with acetone to remove oligomers. GPC analysis performed by using a Tosoh TSK-GEL G3000HHR column (7.8 mm × 30 cm) and THF as a solvent indicated M_w = 5647 based on polystyrene calibration with a polydispersity of 2.0.

Computational Studies. MNDO-PM3 calculations were performed by using version 6.10 of the MOPAC program.[26] INDO/1 calculations were performed by the ZINDO program.[22] These calculations were carried out using the Sony-Tektronix CAChe system.

Acknowledgment. We thank Dr. Takanori Suzuki, Mr. Tomoo Sakimura, and Professor Tsutomu Miyashi of Tohoku University for the preparation of compounds **2a** and **2c** and Professor Noboru Oyama of Tokyo University of Agriculture and Technology for valuable discussions. This work was supported by a Grant-in Aid of Scientific Research from the Ministry of Education, Science and Culture, Japan.

Supplementary Material Available: ^1H NMR spectrum of **3g** (2 pages). This material is contained in libraries on microfiche, immediately follows this article in the microfilm version of the journal, and can be ordered from the ACS; see any current masthead page for ordering information.

(26) Stewart, J. J. P. *QCPE Bull.* **1983**, *3*, 43.

(27) The authors have deposited atomic coordinates for **1a** and **2a** with the Cambridge Crystallographic Data Centre. The coordinates can be obtained, on request, from the Director, Cambridge Crystallographic Data Centre, 12 Union Road, Cambridge, CB2 1EZ, UK.